encit 2020

ABCM Associação Brasileira de Engenharia e Ciências Mecânicas

18th Brazilian Congress of Thermal Sciences and Engineering
November 16–20, 2020 (Online)

ENC-2020-0451
NUMERICAL STUDY OF THE PSEUDOPOTENTIAL LATTICE BOLTZMANN METHOD THERMODYNAMIC CONSISTENCY FOR FLAT INTERFACES

Luiz Eduardo Czelusniak
Luben Cabezas-Gómez
Escola de Engenharia de São Carlos, Universidade de São Paulo, Avenida Trabalhador São-Carlense, 400 - Parque Arnold Schimidt São Carlos - SP, 13566-590, Brazil
Alexander J. Wagner
Department of Physics, North Dakota State University, Fargo, North Dakota 58108, USA
luiz.czelusniak@usp.br, lubencg@sc.usp.br

Abstract. *The pseudopotential lattice Boltzmann method has growing as an alternative tool for multiphase simulations in respect with traditional CFD (Computational Fluid Dynamics) techniques. Originally, this method suffered with lack of thermodynamic consistency. Based on the theoretical solution of a planar interface, authors proposed a correction term for the pseudopotential method to provide improved thermodynamic consistency. By adjusting the coefficient of this term, it is possible to control the shape of the coexistence curve. Although these corrections come from a well defined theory, in most works is observed that thermodynamic consistency is obtained by adjusting the correction terms empirically. In this work it is developed a numerical routine to determine the theoretical value of this coefficient. Then, this coefficient obtained from theory is used in the lattice Boltzmann simulation instead of obtaining it by empirical means. This procedure allows a direct comparison of the lattice Boltzmann solution with theoretical results which make evident the presence of discretization errors that can make the numerical solution deviates from the expected behavior. The procedure is tested for two different equations of state (EOS), for the Carnahan-Starling EOS the theoretical coexistence curve was determined within* 1.5×10^{-3} *% of accuracy, while for the Peng-Robinson EOS the higher deviation was smaller then* 0.12 *%. Also, it was noted that for both cases at lower reduced temperatures a small change in the coefficient that controls the coexistence curve promotes a large variation in the phase densities. After that the theoretical coexistence curve of the pseudopotential lattice Boltzmann method was compared with the results from numerical simulation in order to quantify the discretization errors. It was discovered that the gas phase densities obtained by numerical simulation deviates almost* 140 *% then the predicted by the theory for reduced temperature close to* $T_r = 0.5$ *which suggest that discretization errors play an important role for small reduced temperatures.*

Keywords: *Lattice Boltzmann Method, Pseudopotential Method, Thermodynamic Consistency*

1. INTRODUCTION

The application of the lattice Boltzmann method (LBM) to fluid dynamic simulation has gained much attention in the scientific literature. Despite its complex theoretical background that is related with the kinetic theory of gases, the method results in a simple and computational efficient numerical scheme. These advantages are related with the fact that the LBM is similar to pseudocompressible methods and does not involve the solution of the Poisson equation which can take a lot of computational effort (Krüger *et al.*, 2017). Also, the LBM consists in an explicit algorithm where the heaviest computations are local (restricted to within nodes), making it appropriate to parallel computation (Krüger *et al.*, 2017).

The lattice Boltzmann method can also be applied in the simulation of complex multiphase systems. He *et al.* (1998) developed a method to simulate nonideal gases based on an interparticle interaction using a mean field treatment. Other models were proposed later as (Lee and Lin, 2005; Lee and Fischer, 2006). Wagner (2006) performed an equilibrium analysis and identified the higher-order terms that lead to a lack of thermodynamic consistency in forcing methods. Kikkinides *et al.* (2008) did a comprehensive analysis of standard discretization schemes used in LB models applied in nonideal gases and observed important shortcomings in interface properties indicating lack of thermodynamic consistency in such models. By using a LBM scheme with sufficient order of accuracy Siebert *et al.* (2014) were able to obtain consistent thermodynamic behavior.

One of the most popular extensions of the LBM to simulate multiphase phenomena is the pseudopotential method (Shan and Chen, 1993, 1994). It consists in the introduction of an interaction force that is computed in each node as a function of the node and neighbor nodes density and pressure (computed using an equation of state). This force is capable

of inducing the formation of multiple phases in a fluid. The advantage of this procedure is that it maintain the simplicity and computational efficiency of the LBM even to simulate complex phenomena as multiphase flows. As the multiple phases exists due to an interaction force, it is not necessary to track the interface, which can reduce the computational efficiency of the method.

Besides all the advantages, the original pseudopotential formulation had some drawbacks. The phase densities obtained with the method were different from the ones obtained by applying the Maxwell equal area rule in the equation of state used to compute the interaction force. In this way, the method lack thermodynamic consistency. Shan (2008) correctly derived the equations that define the phase densities of the pseudopotential method for a planar interface problem based on the macroscopic pressure tensor. Later Li *et al.* (2012) added a suitable term into the pressure tensor, which would affect the coexistence curve of the method. By controlling a coefficient that was multiplying this term, the phase densities could be adjusted to approximate the ones given by the condition of thermodynamic consistency. For comprehension, in the rest of the work this coefficient will be called ϵ parameter.

The correct value of ϵ can be theoretically obtained by solving the equations that rule the planar interface problem (Shan, 2008). But in most lattice Boltzmann works, it seems that the ϵ parameter is found "empirically" to match the planar interface coexistence curve with simulation results instead of theoretically obtain its value. This procedure can hidden discretization errors which can deviate the simulation results from expected behaviour. In this work, the goal is to develop a numerical routine to precisely obtain the parameter value that matches the theoretical pseudopotential coexistence curve with the thermodynamic consistent coexistence curve for the same equation of state. The first step is to explicitly determine an approximation for ϵ and then use this first approximation in an iterative procedure to calculate the correct value that solves the planar interface problem to any desired accuracy. With the knowledge of this ϵ, that matches the theoretical coexistence curves, a numerical study is carried out to compare the theoretical results with the ones obtained by the actual pseudopotential simulation.

2. METHODS

2.1 The lattice Boltzmann method

The hydrodynamic model is given by the lattice Boltzmann equation (LBE). This equation describes the time evolution of the particle distribution function f_i:

$$f_i(t+1, \mathbf{x}+\mathbf{c}_i) - f_i(t, \mathbf{x}) = \Omega_i(f_i, f_i^{eq}) + S_i, \tag{1}$$

where t and $\mathbf{x}$ are the time and space coordinates, respectively. Each distribution function is related with a lattice velocity $\mathbf{c}_i$. For two-dimensional simulations the standard D2Q9 lattice is used (Krüger *et al.*, 2017). The term $\Omega_i(f_i, f_i^{eq})$ in the right-hand side of Eq. (1) is called the collision operator and it is in general a function of f_i and of the equilibrium distribution function f_i^{eq}. The single-relaxation time collision operator, also known as BGK operator, is the simplest form of $\Omega_i(f_i, f_i^{eq})$ that permits to solve the Navier-Stokes equations:

$$\Omega_i(f_i, f_i^{eq}) = -\frac{1}{\tau}(f_i - f_i^{eq}). \tag{2}$$

where the parameter τ is the relaxation time. The distribution function f_i^{eq} is given by the following expression:

$$f_i^{eq} = w_i\left(\rho + \frac{c_{i\alpha}}{c_s^2}\rho u_\alpha + \frac{(c_{i\alpha}c_{i\beta} - c_s^2\delta_{\alpha\beta})}{2c_s^4}\rho u_\alpha u_\beta\right), \tag{3}$$

where w_i are the weights related with the lattice velocities $\mathbf{c}_i$ and c_s is the lattice sound speed. The standard values of w_i and c_s for the D2Q9 set can be found in a LBM textbook (Krüger *et al.*, 2017). The last term in the right-hand side of Eq. (1) is the forcing scheme and it is responsible for adding the effect of an external force, F_α, into the LBE. One of the most used forcing scheme was developed by Guo *et al.* (2002):

$$S_i = \left(1 - \frac{1}{2\tau}\right)w_i\left[\frac{(c_{i\alpha} - u_\alpha)}{c_s^2} + \frac{(c_{i\beta}u_\beta)}{c_s^4}c_{i\alpha}\right]F_\alpha, \tag{4}$$

The fluid density ρ and velocity $\mathbf{u}$ can be obtained from the distribution function moments:

$$\rho = \sum_i f_i, \quad \rho\mathbf{u} = \sum_i f_i\mathbf{c}_i + \frac{\mathbf{F}}{2}. \tag{5}$$

The momentum conservation equations resulting from this numerical scheme can be obtained with the aid of a Chapman-Enskog analysis or a recursive substitution (Holdych *et al.*, 2004; Lycett-Brown and Luo, 2015). For the BGK collision operator:

$$\partial_t\rho + \partial_\alpha(\rho u_\alpha) = 0, \tag{6}$$

$$\partial_t(\rho u_\alpha) + \partial_\beta(\rho u_\alpha u_\beta) = -\partial_\beta(\rho c_s^2 \delta_{\alpha\beta}) + \partial_\beta\left(\mu(\partial_\beta u_\alpha + \partial_\alpha u_\beta)\right) + F_\alpha, \tag{7}$$

the dynamic viscosity μ is dependent on the relaxation time $\mu = \rho c_s^2(\tau - 0.5)$.

2.2 The pseudopotential method

The pseudopotential method has its origin with the interaction force proposed by Shan and Chen (1993). The original Shan and Chen formulation suffer from the described drawbacks. In this work it was used the procedure proposed by Li *et al.* (2012). The force is computed in the same way as in the original Shan and Chen formulation:

$$F_\alpha^{SC} = -G\psi(\mathbf{x}) \sum_i w(|\mathbf{c}_i|^2)\psi(\mathbf{x} + \mathbf{c}_i)c_{i\alpha}, \tag{8}$$

the weights $w(|\mathbf{c}_i|^2)$ are $w(1) = 1/3$ and $w(2) = 1/12$. The effective density ψ is used to add a new equation of state P_{EOS} to the system:

$$\psi(\rho, T) = \sqrt{\frac{2\left(P_{EOS}(\rho, T) - c_s^2\rho\right)}{Gc^2}}, \tag{9}$$

according to Li *et al.* (2012) the force given by Eq. (8) should be implemented by a modified version of the Guo *et al.* forcing scheme:

$$S_i = \left(1 - \frac{1}{2\tau}\right) w_i \left[\frac{(c_{i\alpha} - u'_\alpha)}{c_s^2} + \frac{(c_{i\beta}u'_\beta)}{c_s^4} c_{i\alpha}\right] F_\alpha, \tag{10}$$

where:

$$u'_\beta = u_\beta + \sigma \frac{F_\beta}{(\tau - 0.5)\psi^2}, \tag{11}$$

the fluid density ρ and velocity $\mathbf{u}$ are still computed using Eq. (5). The parameter σ is used to adjust the shape of the coexistence curve. Incorporating all the resulting source terms into the pressure tensor, the Li *et al.* procedure results in the following momentum conservation equation:

$$\partial_t(\rho u_\alpha) + \partial_\beta(\rho u_\alpha u_\beta) = -\partial_\beta p_{\alpha\beta} + \partial_\beta\left(\mu(\partial_\beta u_\alpha + \partial_\alpha u_\beta)\right), \tag{12}$$

where the pressure tensor $p_{\alpha\beta}$ is given by the following relation:

$$p_{\alpha\beta} = \left(\rho c_s^2 + \frac{Gc^2}{2}\psi^2 + \frac{Gc^4}{12}\psi\partial_\gamma\partial_\gamma\psi\right)\delta_{\alpha\beta} + \frac{Gc^4}{6}\psi\partial_\alpha\partial_\beta\psi + 2G^2c^4\sigma(\partial_\alpha\psi)(\partial_\beta\psi). \tag{13}$$

where c is the lattice constant (Li *et al.*, 2012), and for nearest neighbor interactions $c = 1$ (Shan, 2008). The Shan and Chen force, Eq. (8), is a discrete force term. In order to obtain a continuous version for the pressure tensor, during the analysis, the Taylor series expansions used to convert the discrete terms into continuous terms are truncated in a certain degree of accuracy. According to Shan (2008), for two phases separated by a planar interface, the phase densities can be calculated from the continuous version of the pressure tensor, Eq. (13), using the following relation:

$$\int_{\rho_g}^{\rho_l} \left(p_0 - \rho c_s^2 - \frac{Gc^2}{2}\psi^2\right) \frac{\dot{\psi}}{\psi^{1+\epsilon}} d\rho = \int_{\rho_g}^{\rho_l} \left(p_0 - P_{EOS}\right) \frac{\dot{\psi}}{\psi^{1+\epsilon}} d\rho = 0, \tag{14}$$

in the case of the Li *et al.* (2012) forcing scheme ϵ is related to σ by $\epsilon = -48G\sigma/3$. The Maxwell equal area rule is given by:

$$\int_{\rho_g}^{\rho_l} \left(p_0 - P_{EOS}\right) \frac{d\rho}{\rho^2} = 0. \tag{15}$$

By comparing Eqs. (14) and (15), it is concluded that the thermodynamic consistency condition can be approximated by changing the value of ϵ. In this work, two equations of state are used. The Carnahan-Starling (C-S) EOS is given by the following relation:

$$P_{EOS} = \rho RT \frac{1 + b\rho/4 + (b\rho/4)^2 - (b\rho/4)^3}{(1 - b\rho/4)^3} - a\rho^2, \tag{16}$$

with $a = 0.4963R^2T_c^2/p_c$ and $b = 0.18727RT_c/p_c$. The parameter R is the ideal gas constant and in the international unit system it is given by $R = 8.3145 J.mol^{-1}K^{-1}$. The C-S EOS is a two parameters equation of state. Which means that given T_c and P_c, the parameters a and b will be determined. In this way, by expressing the C-S EOS in terms of the reduced variables, any fluid will be expressed by the same equation of state. This allow us, to arbitrary change the unit system of the parameters R, a and b. Then the fluid properties in this new unit system can be related with the real fluid properties by the requirement that the reduced properties ρ_R, p_R and T_R should be the same in every unit system. Following Yuan and Schaefer (2006), it is used $a = 1$, $b = 4$ and $R = 1$. And also, it will be tested the Peng-Robinson (P-R) EOS:

$$P_{EOS} = \frac{\rho RT}{1 - b\rho} - \frac{a\alpha(T)\rho^2}{1 + 2b\rho - b^2\rho^2}, \tag{17}$$

$$\alpha(T) = \left[1 + (0.37464 + 1.54226\omega - 0.26992\omega^2)(1 - \sqrt{T/T_C})\right]^2, \tag{18}$$

with $a = 0.45724R^2T_c^2/p_c$ and $b = 0.0778RT_c/p_c$. The acentric factor ω is an additional parameter that give some flexibility in modeling different fluids. Again, following Yuan and Schaefer (2006) it is used $a = 2/49$, $b = 2/21$ and $R = 1$. It will be used the acentric factor for water $\omega = 0.344$.

3. PROPOSED PROCEDURE

In order to make the phase densities obtained by the lattice Boltzmann method equivalent to the ones obtained by the Maxwell rule, it is only necessary an ϵ value that satisfy Eq. (14) for the desired densities. This equation can be solved by a root finder technique until reach into an ϵ value that solves the equation inside a desired tolerance. The Newton method is a simple numerical procedure that can be used. This method requires an initial guess for ϵ. This section is divided in two parts. In the first, it is discussed how to obtain an initial approximation for ϵ and, in the second part, it is described the rest of the numerical routine to obtain an accurate value for this parameter.

3.1 Obtaining an initial approximation

A more strict condition that would guarantee thermodynamic consistency was pointed out by Lycett-Brown and Luo (2015):

$$\frac{\dot{\psi}}{\psi^{1+\epsilon}} d\rho \propto \frac{d\rho}{\rho^2}, \tag{19}$$

this equation is not expected to be satisfied, but it can be used as an initial approximation. Assuming that Eq. (19) is valid it can be integrated to obtain the following relation:

$$\rho = K\psi^{\epsilon}, \tag{20}$$

with the assumption that $\epsilon \neq 0$. This equation can also be written in the following form:

$$\ln\rho = \epsilon \ln\psi + \ln K, \tag{21}$$

which means the ϵ is the angular coefficient given by the plot with $\ln\psi$ in the horizontal axis and $\ln\rho$ in the vertical axis. Since ψ is also a function of the density and temperature $\psi = \psi(\rho, T)$, it is possible to compute the following error function:

$$Error(\epsilon, K, T) = \frac{\int_{\rho_g}^{\rho_l} \left[\ln\rho - \epsilon\ln\psi(\rho,T) - \ln K\right]^2 d\rho}{\rho_l - \rho_g} \approx \frac{\sum_i \left[\ln\rho_i - \epsilon\ln\psi(\rho_i,T) - \ln K\right]^2 \Delta\rho}{\rho_l - \rho_g}, \tag{22}$$

where $\Delta\rho = (\rho_l - \rho_g)/n$, with n being the number of nodes used to perform the numerical integration. The densities ρ_g and ρ_l are the densities obtained by applying the Maxwell rule to the desired equation of state. In this work, it was used $n = 100$. Now, it is possible to find the ϵ value that minimizes the error function:

$$\epsilon = \frac{\sum_i x_i(y_i - \bar{y})}{\sum_i x_i(x_i - \bar{x})};\ \bar{x} = \sum_i \frac{x_i}{n};\ \bar{y} = \sum_i \frac{y_i}{n};\ x_i = \ln\psi(\rho_i, T);\ y_i = \ln\rho_i, \tag{23}$$

and this value of ϵ will be used as an initial guess to the Newton method.

3.2 Using the Newton method

The Newton method requires the definition of an error function to be minimized. In this work, it is adopted the following function:

$$F_{error}(\epsilon, T) = \int_{\rho_g}^{\rho_l} (p_0 - P_{EOS}) \frac{\dot{\psi}}{\psi^{1+\epsilon}} d\rho, \tag{24}$$

in each time step a new value of ϵ is computed by $\epsilon^{new} = \epsilon^{old} + \Delta\epsilon$, until $F_{error}(\epsilon^{new}, T) < tol_1$ and $\Delta\epsilon < tol_2$ with tol_1 and tol_2 being two specified tolerances. In this work it is used $tol_1 = tol_2 = 10^{-10}$. The step $\Delta\epsilon$ is given as follows:

$$\Delta\epsilon = -F_{error}(\epsilon, T) / \frac{\partial F_{error}(\epsilon, T)}{\partial \epsilon} = \frac{\int_{\rho_g}^{\rho_l} (p_0 - P_{EOS}) \frac{\dot{\psi}}{\psi^{1+\epsilon}} d\rho}{\int_{\rho_g}^{\rho_l} (p_0 - P_{EOS}) \frac{\dot{\psi} ln\psi}{\psi^{1+\epsilon}} d\rho}, \tag{25}$$

the integrals in the above expression are computed numerically using the Simpson's rule (Atkinson, 2008).

4. NUMERICAL RESULTS

4.1 Carnahan-Starling equation of state

In Fig. (1a) it is shown the results of the initial guess of ϵ obtained by solving Eq. (23) for the C-S EOS in a range of reduced temperatures varying between 0.5 and 1. These values are used to obtain the density profile that solve Eq. (14). The coexistence curve obtained for the initial guess of ϵ is shown in Fig. (1b) and the relative error of the theoretical pseudopotential gas densities in comparison with the ones given by the Maxwell rule is shown in Fig. (1c). It is observed that the initial guess provide a relative good adjustment for the pseudopotential coexistence curve with maximum error smaller than 14% in the range of reduced temperatures between 0.5 and 1.

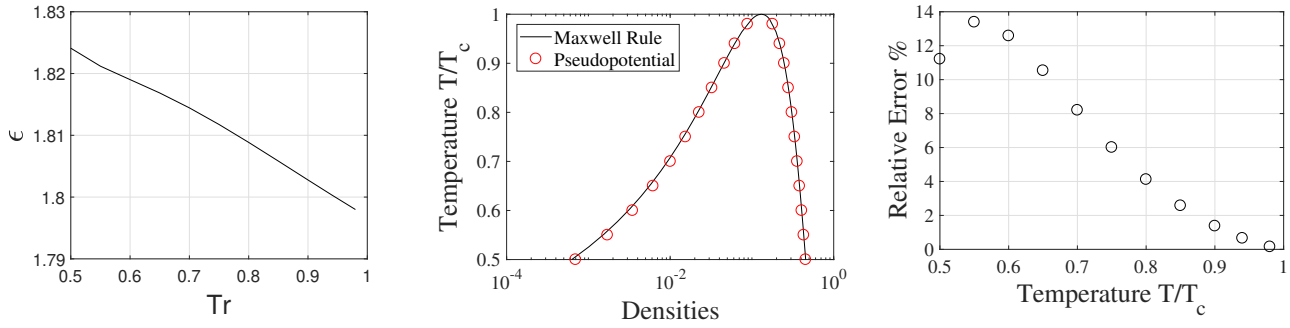

(a) (b) (c)

Figure 1: (a) Values of the approximated ϵ for each reduced temperature $T_r = T/T_c$ for the C-S EOS. (b) Comparison between the coexistence curve given by the Maxwell rule for the C-S EOS with the theoretically predicted phase densities for the pseudopotential method considering the approximated ϵ values. (c) Relative error between the gas density given by the Maxwell rule with the theoretical pseudopotential densities considering the approximated ϵ values.

Next, the approximated value of ϵ is used as an initial condition for the Newton Method. By solving Eq. (25) until the desired tolerance, it is obtained the results for ϵ shown in Fig. (2a). These values are used in Eq. (14) to obtain the theoretical pseudopotential density profile shown in Fig. (2b). The relative error of the gas densities is much smaller now with maximum error smaller than 1.5×10^{-3}. It can be observed that the error grows significantly when the temperature goes toward $T_r = 0.5$. This is happening due to the fact that the gas densities became very small at lower reduced temperature, and they are not computed with the same number of significant digits as the densities for higher temperatures. In this way, to obtain a higher precision for lower temperatures it is necessary to increase the number of significant digits in computations of the densities. It is concluded that the proposed procedure can correctly find the values of the ϵ that provides thermodynamic consistent densities for the pseudopotential method in flat interfaces using the C-S EOS.

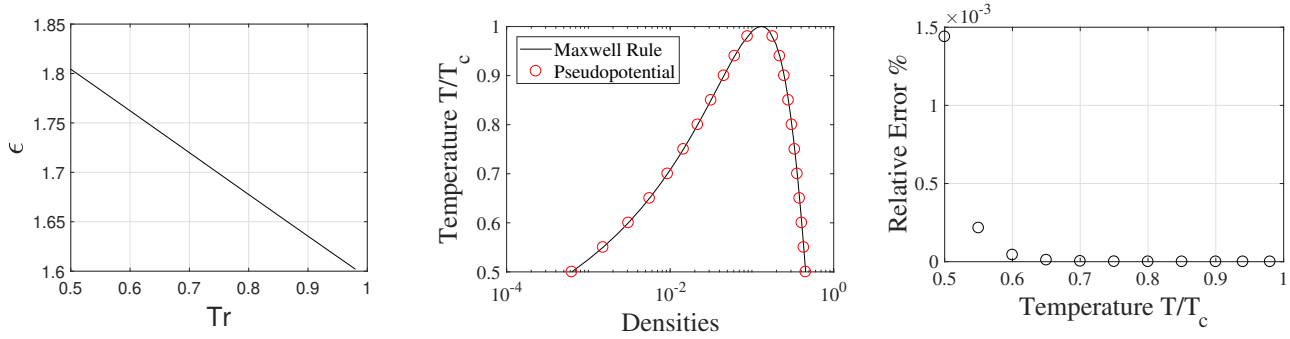

(a) (b) (c)

Figure 2: (a) Actual ϵ values obtained with the Newton method for each reduced temperature $T_r = T/T_c$ for the C-S EOS. (b) Comparison between the coexistence curve given by the Maxwell rule for the C-S EOS with the theoretically predicted phase densities for the pseudopotential method considering the actual ϵ values. (c) Relative error between the gas density given by the Maxwell rule with the theoretical pseudopotential densities considering the actual ϵ values.

4.2 Peng-Robinson equation of state

In Fig. (3a) it is shown the results of the initial guess of ϵ obtained by solving Eq. (23) for the P-R EOS in a range of reduced temperatures varying between 0.5 and 1. These values are used to obtain the density profile that solve Eq. (14). The coexistence curve obtained for the initial guess of ϵ is shown in Fig. (3b) and the relative error of the theoretical pseudopotential densities in comparison with the ones given by the Maxwell rule is shown in Fig. (3c). It is observed that the initial guess provide a relative good adjustment for the pseudopotential coexistence curve with maximum error smaller then 12 % in the range of reduced temperatures between 0.5 and 1.

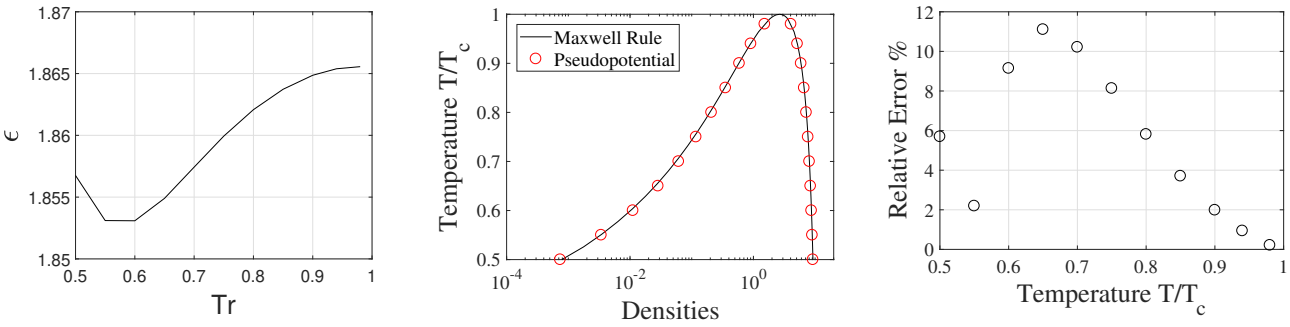

(a) (b) (c)

Figure 3: (a) Values of the approximated ϵ for each reduced temperature $T_r = T/T_c$ for the P-R EOS. (b) Comparison between the coexistence curve given by the Maxwell rule for the P-R EOS with the theoretically predicted phase densities for the pseudopotential method considering the approximated ϵ. (c) Relative error between the gas density given by the Maxwell rule with the theoretical pseudopotential densities considering the approximated ϵ values.

Next, the approximated value of ϵ is used as an initial condition for the Newton Method. By solving Eq. (25) until the desired tolerance, it is obtained the results for ϵ shown in Fig. (4a). These values are used in Eq. (14) to obtain the theoretical pseudopotential density profile shown in Fig. (4b). In Fig. (4c) it is possible to see the relative error. All errors are now bellow 0.12%. It is concluded that the proposed procedure can correctly find the values of the ϵ that provides thermodynamic consistency densities for the pseudopotential method in flat interfaces using the P-R EOS. An interesting behavior, that also happened for the C-S EOS, is observed. Comparing Figs. (3a) and (4a) it can be seen that the largest variation between the initial guess of ϵ and the actual value of ϵ happened for the smaller, in module, reduced temperatures. Which means that the initial guess procedure predicted with less accuracy the ϵ value for these smaller T_r. But when it is observed the relative error of the predicted densities with the initial guess, Fig. (3c), it is concluded that the predicted densities for higher reduced temperatures are closer to the actual densities than those predicted for lower reduced temperatures. These results means that when the reduced temperature is lower, a small change in ϵ promotes a large variation in the phase densities.

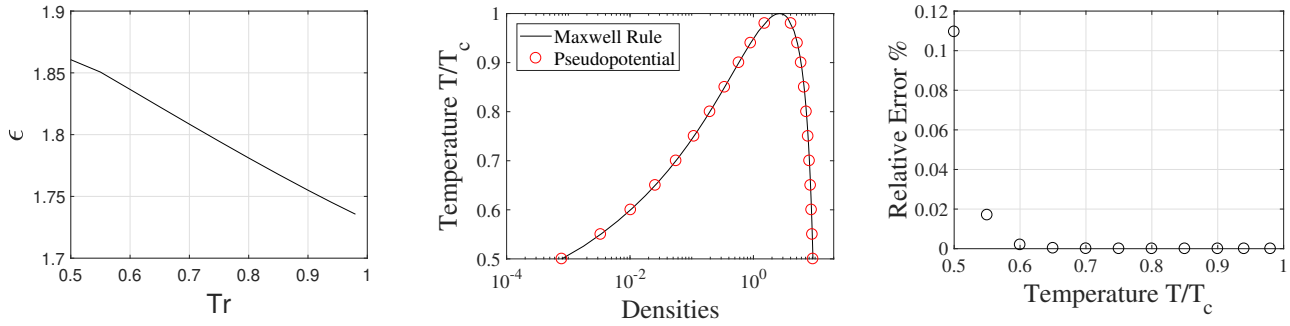

(a) (b) (c)

Figure 4: (a) Values of the approximated ϵ for each reduced temperature $T_r = T/T_c$ for the P-R EOS. (b) Comparison between the coexistence curve given by the Maxwell rule for the P-R EOS with the theoretically predicted phase densities for the pseudopotential method considering the approximated ϵ values. (c) Relative error between the gas density given by the Maxwell rule with the theoretical pseudopotential densities considering the approximated ϵ values.

4.3 Comparison between theoretical and numerical solution

The theoretical coexistence curves shown in the previous section were obtained by means of Eq. (14) which is derived based on the pressure tensor defined by Eq. (13). As discussed before, this continuous form of the pressure tensor is obtained from the discrete pseudopotential method by truncating the Taylor series expansion of the discrete terms. Which means that this expression is an approximation of the actual behavior of the pseudopotential method which also is affected by higher order discretization errors. For comprehensive purposes the results shown in the previous section will be called "theoretical coexistence curve" of the pseudopoential method for a planar interface and the results from the numerical simulation using the lattice Boltzmann method will be called "actual coexistence curve".

In order to compare the theoretical results with the actual results, numerical simulation using the Li *et al.* (2012) pseudopotential approach is performed. The Shan and Chen force, Eq. (8), is solved using the definition of effective density given by Eq. (9). This force is implemented into the LBE, Eq. (1), using the forcing scheme provided by Eq. (10). For a specific equation of state and a specific temperature the gas and liquid densities are calculated using the Maxwell rule, these densities are used to initialized a one-dimensional density profile of $Nx = 200$ nodes with the function:

$$\rho(x) = \rho_g + \frac{\rho_l - \rho_g}{2}\left[\tanh\frac{2(x-x_1)}{W} - \tanh\frac{2(x-x_2)}{W}\right], \tag{26}$$

where $W = 5$. Also, $x_1 = 0.25Nx$ and $x_2 = 0.75Nx$ are the location of the flat interfaces that separate the liquid and gas regions. The velocity was set as zero everywhere. With the initialization of macroscopic fields, the equilibrium distribution function is determined and the particle distribution function was set as equal to the equilibrium one. The relaxation time was set as $\tau = 1$ and simulations were carried until the following convergence criteria has being obeyed:

$$\frac{\sum \mid [\rho(t) - \rho(t-100)] \mid}{\sum \mid \rho(t) \mid} < 10^{-6}. \tag{27}$$

The theoretical ϵ values obtained with the Newton method are used as an input for Eq. (10). A comparison between the theoretical results with the actual pseudopotential simulation is shown in Fig. (5a) for the C-S EOS. Results show a good agreement until $T_r = 0.7$, as can be observed in Fig. (5b). For smaller reduced temperatures, the relative error between the gas phase density start to increase and became very significant when $T_r = 0.5$ is reached. These results means that for small reduced temperatures the discretization errors play an important role. The same behavior is observed for the the P-R EOS, Fig. (6). In this case it was observed that simulations got unstable for reduce temperatures lower then $T_r = 0.6$. The relative error of the gas phase between theoretical and numerical results are shown in Fig. (6b). It can be seen a good agreement until $T_r = 0.8$, and for lower temperatures the error start to increase becoming very significant for $T_r = 0.6$.

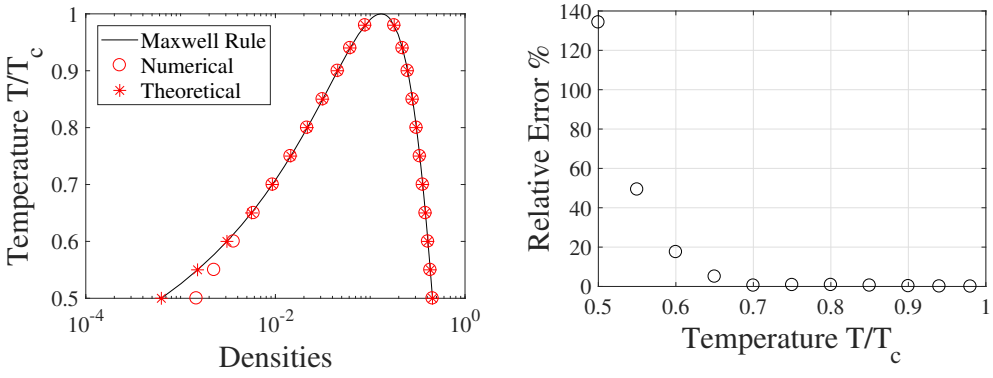

(a) (b)

Figure 5: (a) Comparison between the theoretical phase densities for the C-S EOS for the pseudopotential method obtained by solving Eq. (14) with the ϵ values obtained in Section 4. with the actual results from numerical simulation. (b) Relative error of the gas phase densities between the theoretical and numerical results.

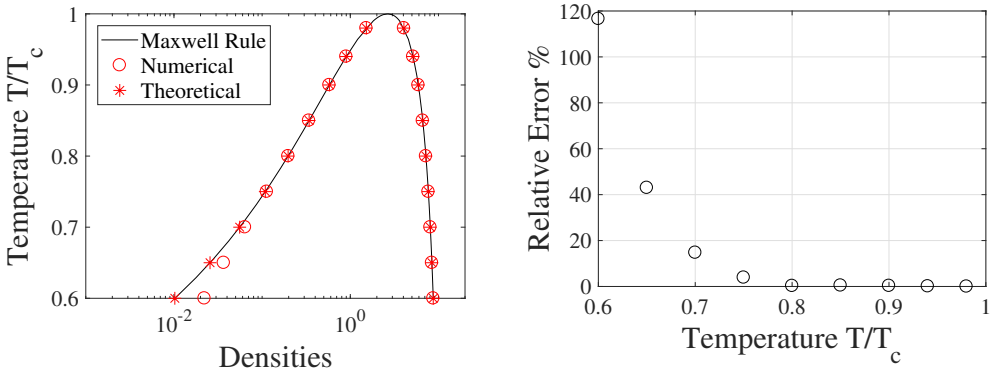

(a) (b)

Figure 6: (a) Comparison between the theoretical phase densities for the P-R EOS for the pseudopotential method obtained by solving Eq. (14) with the ϵ values obtained in Section 4. with the actual results from numerical simulation. (b) Relative error of the gas phase densities between the theoretical and numerical results.

5. CONCLUSION

In this work, it was proposed a procedure to determine the ϵ parameter that adjust the coexistence curve resultant from the theoretical pseudopotential pressure tensor. The procedure consists in two parts, the first one is an explicit way to obtain the ϵ parameter, but only as an approximation. In the second part, this initial approximation is used in the Newton root find technique to obtain a better approximation to ϵ with any desired degree of accuracy. The procedure was tested for two equation of state, the Carnahan-Starling (C-S) and the Peng-Robinson (P-R). The method showed good results for both cases. Later, with the knowledge of the theoretical pseudopotential coexistence curve, it was performed a comparison between the results obtained from the theoretical pressure tensor with the actual pseudopotential simulation. It was observed that simulation agrees with theory for higher reduced temperatures, but deviations were observed when the temperature was decreased. This happened because the theory of the pseudopotential method is based on the differential equations obtained by the truncation of the Taylor series expansion of the discrete numerical method. In this way, the higher order discretization error of the numerical scheme that are not taken into account in the theoretical pressure tensor promotes deviations in the observed results when the reduced temperature is small and density ratios are large.

6. ACKNOWLEDGEMENTS

The authors acknowledge the support received from CNPq (National Council for Scientific and Technological Development, processes 304972/2017-7 and 431782/2018-0) and FAPESP (São Paulo Foundation for Research Support, 2016/09509-1 and 2018/09041-5), for developing research that have contributed to this study.

7. REFERENCES

Atkinson, K.E., 2008. *An introduction to numerical analysis*. John wiley & sons.

Guo, Z., Zheng, C. and Shi, B., 2002. "Discrete lattice effects on the forcing term in the lattice boltzmann method". *Physical Review E*, Vol. 65, No. 4, p. 046308.

He, X., Shan, X. and Doolen, G.D., 1998. "Discrete boltzmann equation model for nonideal gases". *Physical Review E*, Vol. 57, No. 1, p. R13.

Holdych, D.J., Noble, D.R., Georgiadis, J.G. and Buckius, R.O., 2004. "Truncation error analysis of lattice boltzmann methods". *Journal of Computational Physics*, Vol. 193, No. 2, pp. 595–619.

Kikkinides, E., Yiotis, A., Kainourgiakis, M. and Stubos, A., 2008. "Thermodynamic consistency of liquid-gas lattice boltzmann methods: Interfacial property issues". *Physical Review E*, Vol. 78, No. 3, p. 036702.

Krüger, T., Kusumaatmaja, H., Kuzmin, A., Shardt, O., Silva, G. and Viggen, E.M., 2017. "The lattice boltzmann method". *Springer International Publishing*, Vol. 10, pp. 978–3.

Lee, T. and Fischer, P.F., 2006. "Eliminating parasitic currents in the lattice boltzmann equation method for nonideal gases". *Physical Review E*, Vol. 74, No. 4, p. 046709.

Lee, T. and Lin, C.L., 2005. "A stable discretization of the lattice boltzmann equation for simulation of incompressible two-phase flows at high density ratio". *Journal of Computational Physics*, Vol. 206, No. 1, pp. 16–47.

Li, Q., Luo, K.H. and Li, X.J., 2012. "Forcing scheme in pseudopotential lattice boltzmann model for multiphase flows". *Physical Review E*, Vol. 86, No. 1, p. 016709.

Lycett-Brown, D. and Luo, K.H., 2015. "Improved forcing scheme in pseudopotential lattice boltzmann methods for multiphase flow at arbitrarily high density ratios". *Physical Review E*, Vol. 91, No. 2, p. 023305.

Shan, X., 2008. "Pressure tensor calculation in a class of nonideal gas lattice boltzmann models". *Physical Review E*, Vol. 77, No. 6, p. 066702.

Shan, X. and Chen, H., 1993. "Lattice boltzmann model for simulating flows with multiple phases and components". *Physical review E*, Vol. 47, No. 3, p. 1815.

Shan, X. and Chen, H., 1994. "Simulation of nonideal gases and liquid-gas phase transitions by the lattice boltzmann equation". *Physical Review E*, Vol. 49, No. 4, p. 2941.

Siebert, D., Philippi, P. and Mattila, K., 2014. "Consistent lattice boltzmann equations for phase transitions". *Physical Review E*, Vol. 90, No. 5, p. 053310.

Wagner, A., 2006. "Thermodynamic consistency of liquid-gas lattice boltzmann simulations". *Physical Review E*, Vol. 74, No. 5, p. 056703.

Yuan, P. and Schaefer, L., 2006. "Equations of state in a lattice boltzmann model". *Physics of Fluids*, Vol. 18, No. 4, p. 042101.

8. RESPONSIBILITY NOTICE

The authors are solely responsible for the printed material included in this paper.